Eur Biophys J (2012) 41:663–673
DOI 10.1007/s00249-012-0842-4

ORIGINAL PAPER

EBSA
Biophysics in Europe

FTIR spectroscopic study of molecular organization of the antibiotic amphotericin B in aqueous solution and in DPPC lipid monolayers containing the sterols cholesterol and ergosterol

Mariusz Gagoś · Marta Arczewska

Received: 30 March 2012 / Revised: 29 June 2012 / Accepted: 10 July 2012 / Published online: 26 July 2012

Abstract Langmuir monolayers of amphotericin B (AmB) were investigated by recording π–A isotherms under different pH conditions. To gain a better insight into antibiotic–membrane interactions they were monitored by use of the ATR-FTIR spectroscopy. It was observed for AmB monolayers that the limiting molecular area was larger at high than at neutral pH. Analysis of FTIR spectra at different pH revealed substantial differences, depending on ionic state, for different orientations of AmB molecules. These results enable better understanding of the participation of functional groups in the interactions between AmB and sterol-containing DPPC membranes. AmB molecules incorporated into two-component lipid monolayers bind strongly to the ergosterol-rich membrane (maximum penetration surface pressures ca 35 mN/m). The FTIR spectra revealed that the ionic state of AmB and the presence of sterols led to changes in membrane fluidity and molecular packing of the AmB molecules in the lipid membranes. These investigations should be further investigated to discover the molecular mechanism responsible for the mode of action AmB in biological systems.

Keywords Amphotericin B · Langmuir monolayers · Langmuir–Blodgett technique · FTIR spectroscopy

M. Gagoś (✉) · M. Arczewska
Department of Biophysics, University of Life Sciences in Lublin, Akademicka 13, 20-950 Lublin, Poland
e-mail: mariusz.gagos@up.lublin.pl

M. Gagoś
Department of Cell Biology, Institute of Biology and Biotechnology, Maria Curie–Skłodowska University, 20-033 Lublin, Poland

Introduction

Opportunistic systemic fungal infections are increasing. This is connected with the increasing number of immunocompromised patients belonging to infection risk groups, for example HIV-positive and post-operative surgical patients. Amphotericin B (AmB) is one of the oldest polyene antibiotics, and has been clinically used as an antimycotic agent for more than 50 years (Gold et al. 1956). Because of its very high activity against a broad range of pathogenic fungi, AmB remains the recommended treatment for serious systemic mycoses, despite its nephrotoxicity and adverse effects (Zotchev 2003). It was proposed in the 1970s that the pharmacological action of AmB is responsible for greater selectivity toward ergosterol–containing fungal cells than toward cholesterol–containing mammalian cells (De Kruijff et al. 1974; Fournier et al. 1998). One common hypothesis is that the molecular action of AmB is based on formation of trans-membrane channels that cause structural and organizational disturbance of membrane barrier function (Hartsel et al. 1993). This contributes to an uncontrolled increase in its permeability to monovalent ions, in particular K^+, and small molecules from the cell (Brajtburg and Bolard 1996).

One of the main factors with relevance both to its chemotherapeutic action and to the suggested trans-membrane pore structure is the function of sterols (Paquet et al. 2002). However, there are a variety of models of formation of membrane channels by AmB, and the detailed molecular mechanisms of these interactions and its porous architecture are still not unambiguously determined. It has been proposed that the sterol molecule could be involved in the construction of these channels. There is much experimental evidence confirming the validity of the so-called sterol hypothesis (Cotero et al. 1998; Hamilton-Miller 1974).

Readio and Bittman (1982) observed that AmB binding constants to ergosterol membranes ($K = 6.9 \times 10^5$ M^{-1}) are greater than those to cholesterol membranes ($K = 5.2 \times 10^5$ M^{-1}). Application of molecular dynamics simulation techniques revealed differences in the sizes of pores formed by AmB molecules in lipid membranes containing sterols; larger diameters were recorded for membranes containing ergosterol. AmB–ergosterol channels were also more stable, because of the presence of a strong network of hydrogen bonds between AmB molecules and subtle differences in the energy of van der Waals interactions (Sternal et al. 2004). It has been proposed that van der Waals interactions (or π–π* electron interactions) between neighbouring AmB chromophores and a lipophilic sterol molecule are responsible for the stability of the AmB–sterol complex (Baran and Mazerski 2002). In this way, the first step of porous structure formation is the so–called primary complex, which, as a result of spontaneous aggregation, creates a proper channel (Baran et al. 2009; Herve et al. 1989; Mazerski et al. 1995). Mazerski et al. (1995) suggest that three different forces participate in the interactions between AmB molecules and sterols:

- *binding forces* between the hydrophobic parts of the drug and sterol molecules;
- *stabilising forces* between the amino group of one molecule of AmB and the carboxyl group of a neighbouring one;
- *orienting forces* between the 3-β-OH group of the sterol and, probably, the OH group of the mycosamine moiety (Baran et al. 2009; Mazerski et al. 1995).

The different affinity of the antibiotic for cholesterol and ergosterol was also demonstrated in studies of two-component monolayers containing AmB formed at the air–water interface. Both sterols affected incorporation of AmB molecules into lipid membranes, but the effect was stronger for the fungal sterol (Barwicz and Tancrede 1997). It has been postulated that the structural differences between sterols may have affect the physical properties of lipid bilayers and, in this way, the mechanism of interaction with AmB molecules (Baginski et al. 1989). It has been suggested that the more rigid molecule of ergosterol has a structure more complementary to the structure of AmB than that of cholesterol, because of the presence of an additional double bond on the side chain and the steroid nucleus. A flat shape and an additional π-electron interaction located at the conformers of the ergosterol molecule causes an increase in local electron density of the side chain of ergosterol (Baginski and Borowski 1997; Baginski et al. 1994; Clejan and Bittman 1985), and an additional methyl group in the ergosterol molecule can induce changes in membrane fluidity and molecular packing of the AmB molecules in the hydrophobic part of the membrane (Gagoś et al. 2005). The results of spectroscopic measurements and the monomolecular layer technique show that the AmB molecules are located mostly in the polar headgroup region, which facilitates their incorporation into the membranes (Gagoś et al. 2005).

Monomolecular layers and the Langmuir–Blodgett technique have been used to investigate the molecular organization of AmB on the surface of the subphase at different pH. In this work we report, for the first time, ATR-FTIR spectra of pure AmB monolayers in different ionic states, depending on the molecular orientation. FTIR spectroscopy was also used to study the interaction of AmB in two-component monolayers containing cholesterol and ergosterol. The main vibrational modes involved in the processes of interaction between AmB and the DPPC/sterol system are the symmetric and asymmetric vibrations of the COO^-, NH_2, and C=O groups (AmB molecule), the O–H stretch, and the mode of PC headgroups.

Materials and methods

Amphotericin B (AmB) in a crystalline form was purchased from Sigma. The AmB was dissolved in deionised (mQ) water, made alkaline (pH 11) by addition of KOH and then centrifuged for 15 min at 15,000×g to remove micro–crystals of the drug still remaining in the sample. The AmB was further purified by HPLC on a YMC C30-coated reversed-phase column (length 250 mm, internal diameter 4.6 mm) with 40 % 2-propanol in H_2O as mobile phase. The final concentration of AmB was calculated from the absorption spectra on the basis of the molar extinction coefficient (0–0 absorption maximum at 408 nm at pH 11) $\varepsilon_{408} = 1.1 \times 10^5$ $M^{-1}cm^{-1}$.

The subphase for each experiment was water filtered through a set of membrane filters (Millipore Express® Plus, 0.22 μm).

Monolayer experiments were performed by use of a Minitrough 2 (KSV Instruments, Finland) placed in a laminar hood purged with N_2 (relative humidity 80 %). Monomolecular layers were formed in a Teflon trough (282 mm × 75 mm) equipped with two symmetric, hydrophilic barriers and a Wilhelmy platinum plate as the surface pressure tensor. Monomolecular layers of the mixture were formed at the air–water interface. After each measurement, the surface was meticulously cleaned. Spreading solutions were deposited on to the water with a Hamilton microsyringe (accuracy ±0.1 μl). The solvent was left to evaporate for 15 min and the monolayers were compressed with a barrier speed of 75 cm^2/min. Each π–isotherm presented in this work is the average from three independent experiments. The subphase temperature (24 ± 1 °C) was controlled by use of a PolyScience thermocirculator trough.

Monomolecular layers were deposited on to the two sides of a Ge crystal plate by means of the Langmuir–Blodgett technique (L–B films), with a lift speed of 5 mm/min at a computer-controlled surface pressure depending on the experiment. To remove water residues, thin L–B films were placed in a vacuum for 1 h. Second, ATR Ge crystals with monolayers deposited at different pressures were placed in a sample holder in the chamber of FTIR spectrometer.

Infrared absorption spectra were recorded with a 670-IR Varian spectrometer. The attenuated total reflection (ATR) configuration was used with 10 internal reflections of the HATR Ge crystal plate (45° cut). Typically, 25 scans were collected, Fourier-transformed, and averaged for each measurement. Absorption spectra at a resolution of one data point cm^{-1} were obtained in the region between 4,000 and 600 cm^{-1}. The instrument was continuously purged with N_2 gas for 40 min before and during the measurements. The Ge crystal plate was cleaned with ultra pure organic solvents from Sigma–Aldrich. All the experiments were performed at room temperature. Spectral analysis was performed with Grams/AI software from ThermoGalactic Industries (USA).

Results and discussion

One of the most important tasks in this study was characterization, by FTIR spectroscopy, of the effect of pH on the molecular organization of AmB in monomolecular layers formed at the air–water interface. These results are crucial for explanation of the molecular organization of AmB during incorporation into the model membrane system containing sterols. Model diagrams of the different ionic states of the ionisable parts of the AmB molecule are presented in Fig. 1. At pH < 3, dissociation of the carboxyl group is strongly inhibited and the molecule has a positive net charge. At pH > 10, in contrast, the amino group is no longer protonated and the AmB molecule has a negative net charge (Mazerski et al. 1990).

The surface pressure–area (π–A) isotherms of the pure AmB monolayer spread on the aqueous subphase at pH 7 and 11 are shown in Fig. 2. The shape of the π–A isotherm at neutral pH is very similar to those of the isotherms previously reported (Arczewska and Gagoś 2011; Gagoś and Arczewska 2010; Gruszecki et al. 2002; Minones et al. 2001; Saint-Pierre-Chazalet et al. 1988; Seoane et al. 1997, 1998; Sykora et al. 2004). It has the typical plateau indicative of molecular reorientation of AmB molecules from a horizontal to a vertical position on compression (Gagoś and Arczewska 2010; Rey-Gomez-Serranillos et al. 2001; Saint-Pierre-Chazalet et al. 1988; Seoane et al. 1997). For horizontally oriented molecules, the limiting

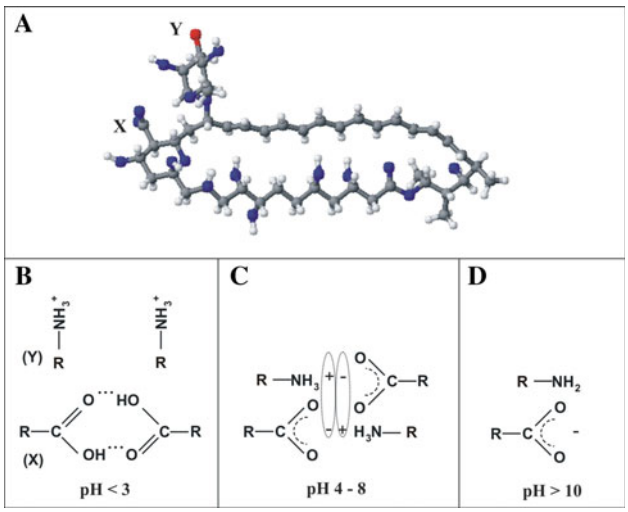

Fig. 1 Structure of amphotericin B (**a**) with the indicated functional groups; X: $–COO^-$, Y: $–NH_3^+$. Schematic hypothetical arrangement of the net electric charge of the molecule at low pH (**b**), in the pH range 4–8 (**c**), at high pH (**d**)

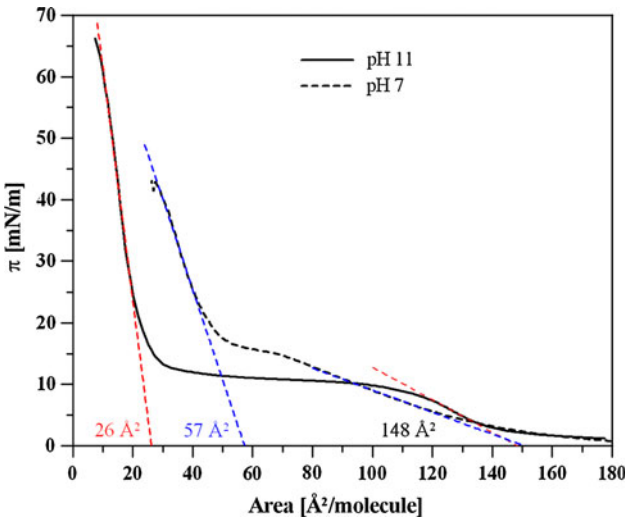

Fig. 2 The surface pressure–area isotherms of AmB spread on water at pH 11 (*solid line*) and at pH 7 (*dashed line*). The linear fits to the linear portions of the isotherms of compression extrapolated to zero surface pressure are indicative of the specific molecular areas in the horizontal position (A_e) and in the vertical position (A_c). Temperature 24 °C

molecular area (148 $Å^2$/molecule) is similar at both pH values. The most remarkable differences were observed in the vertical position. The limiting molecular areas obtained from fitting the isotherms in extremely packed monolayers are: 26.0 and 57 $Å^2$/molecule for AmB at pH 7 and 11. In comparison with the neutral subphase, a weakly visible plateau and a relatively short solid condensed region, which immediately disappears at ca. 43 mN m^{-1}, are observed for monolayers spread on the basic subphase. When AmB molecules are vertically oriented at the

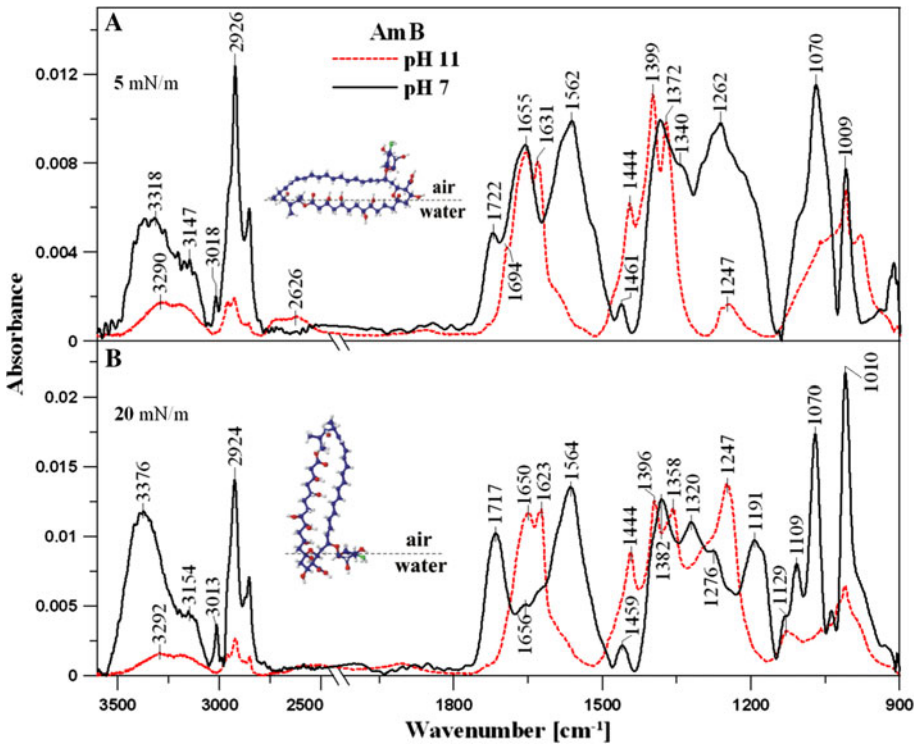

Fig. 3 ATR-FTIR absorption spectra recorded from AmB monolayers at pH 11 (**a**) and pH 7 (**b**). Samples were deposited on the two sides of a Ge crystal plate at 5 mN/m (**a**) and 20 mN/m (**b**). Concentration of AmB in the sample 10^{-6} M. The *insets* show models of reorientation of AmB molecules on the subphase at low and high surface pressures. Temperature 24 °C

interface, the stability of the monolayer is very low, because of the high solubility of the molecules under these conditions. This phenomenon is especially pronounced at pH 11, because at this pH AmB molecules become negatively charged as a result of deprotonation of the carboxyl groups. For this reason, at pH 11 the monolayer has a short solid condensed region, without reaching a real collapse compared with that formed at the neutral pH subphase (66 mN m^{-1}). The limiting molecular area reaches a greater value at high pH than on the neutral-pH subphase and this value is much higher than the expected area of the cross section of AmB (Bonilla-Marin et al. 1991). The experimental results are quite expected from the perspective of electrostatic repulsion, because the total net charge of the AmB molecules becomes negative after deprotonation of the carboxyl group and electrostatic repulsion between molecules will be increased.

Figure 3 shows ATR–FTIR spectra of the AmB monolayers formed at the air–water interface under different pH conditions (11 and 7). The positions of the main AmB absorption bands under the different conditions are listed in Table 1. Detailed analysis and discussion of all bands are given elsewhere (Gagoś and Arczewska 2010; Gagoś et al. 2011). In contrast with our previous studies FTIR spectra were recorded at two surface pressures 5 and 20 mN/m forcing different orientation of AmB molecules (Gagoś et al. 2008b). On the basis of the π–A isotherm, it is known that at a surface pressure of ca 5 mN/m AmB molecules are oriented horizontally (relative to the water surface) (Arczewska and Gagoś 2011; Gagoś and Arczewska 2010). During compression, the AmB molecules change their orientation to vertical at a surface pressure of approximately 15 mN/m (Arczewska and Gagoś 2011; Gagoś and Arczewska 2010; Gruszecki et al. 2002). FTIR spectra of AmB monolayers deposited on the Ge plate by the Langmuir–Blodgett technique from aqueous solution at a surface pressure of 5 mN/m are presented in Fig. 3a. First, it is important to point out that the differences depend on the spectral region between 1,800 and 1,100 cm^{-1}. Information about the AmB conformation may be deduced from the bands assigned to the vibrations of the C=O, C=C, and NH_3^+ groups, which are known to be highly sensitive to reorientation of the drug molecules.

As indicated by the spectra in Fig. 3a, a weak maximum with its centre-wavelength position at 1,722 cm^{-1} is visible at neutral pH whereas there is no spectral intensity at pH 11 (Table 1). According to spectral assignments based on many studies (Gagoś and Arczewska 2010; Gagoś et al. 2005, 2008a), this band is assigned to the vibration of C=O in the protonated form of the –COOH group. As it was mentioned, at neutral pH, most carboxylate groups are partially protonated. Indeed, this is powerfully confirmed at low surface pressure as a result of the appearance of a strong band centred at 1,262 cm^{-1}, characteristic of C–O modes in the protonated carboxyl group. Interestingly, during compression to high surface pressure (Fig. 3b), a spectral shift of this band toward lower frequencies (1,717 cm^{-1}), together with a substantial increase in its

Table 1 Comparison of the location (cm^{-1}) of the IR bands of AmB at pH 7 and pH 11 during compression of the monolayers to surface pressures 5 and 20 mN/m

Wavenumber (cm^{-1})				Assignment[a]
AmB monolayers				
pH 7		pH 11		
5 mN/m	20 mN/m	5 mN/m	20 mN/m	
1009s	1010s	1009w	1010w	δ(C–C–H) for chromophore, γ(–CH) in *trans*-polyene
1070s	1070s	–	–	ν_{as}(C–O)
–	1109	–	–	ν_{as}(C–O–C) for β–glycosidic linkage (C–O–C=O)
–	1129	–	1129	ν(C–O–C) for ester + δ(OH)
–	1191s	–	–	
1262	1276w	1247	1247s	$\delta(-CH_2)$
–	1320	–	1358	$\delta(CH_3) + \delta$(OH)
1372	1382	1399	1396	
1466	–	1444	1444	$\nu_s(-COO^-)$, δ(–CH)
1461	1459	–	–	$\delta_{as}(CH_2, CH_3)$
1562s	1564	–	–	$\delta_s(-NH_3^+) + \nu$(C=C)
–	1623w	1631	1623	$\delta_{as}(-NH_3^+)$
1655s	1656w	1655s	1650	$\nu_{as}(-COO^-)$
–	–	1694w	–	
1722w	1717s	–	–	ν_{as}(C=O) for ester, ν(C=O) for saturated carboxylic group
	2800–3000		$\nu_{s+as}(CH_2, CH_3) + \nu$(CH) in polyene	
3318	3376	3290	3292	ν(–OH), ν(N–H)

[a] ν, stretching mode; δ, bending in plane; γ, bending out of plane; *s* symmetric vibrations, *as* asymmetric vibrations, *s*,*w* strong and weak intensity, respectively

intensity, are observed. The band centred at 1,722 cm^{-1} is coupled with the vibrations of C=O in the ester. The absence of this band at pH 11 might also be associated with enolization of the ester fragment in the AmB molecule or deprotonation of the –COOH (Gagoś et al. 2008a). It might be manifested by appearance of an additional C–H mode located at 1,444 cm^{-1}. At pH 11, because of complete deprotonation, carboxylate groups are mostly transformed into the $-COO^-$ groups, and there is weak intensity in the C=O spectral region (shoulder at 1,694 cm^{-1}) (Gagoś and Arczewska 2010). A pair of intense bands centred at 1,655 and 1,631 cm^{-1} are clearly visible (Gagoś and Arczewska 2010, 2011). This is a direct indication of the asymmetric stretch of the $-COO^-$ group interacting with the interface. During compression to the surface pressure of 20 mN/m, the second band of this pair is shifted toward lower frequencies by 8 cm^{-1} (Fig. 3b). At neutral pH, the amino group is partially deprotonated. This may determine the presence of two different carboxylate asymmetric stretching vibrations as reported in amino acids, one arising from the protonated amino group around 1,630 cm^{-1}, the other from the deprotonated amino at 1,560 cm^{-1}. The bands with a maximum at 1,400 cm^{-1} are assigned to the symmetrical vibration of the $-COO^-$ group. The asymmetric stretching mode shifts gradually to higher wavenumber (1,650 cm^{-1}) as the pH is reduced, presumably because of the effects of intramolecular hydrogen bonding between neighbouring carboxyl groups as the degree of protonation of the AmB molecules increases at lower pH. At pH 7 (Fig. 1c), AmB molecules are zwitterions ($-COO^-$/$-NH_3^+$), which causes their aggregation (Mazerski et al. 1995). This effect is connected with the AmB aggregation process and is related to the interactions between the $-COO^-$ and $-NH_3^+$ groups, which has a strong effect on the changes in vibration frequencies (Gagoś and Arczewska 2010). The broad band ca. 1,560 cm^{-1} contains overlapped lines because of contributions of the $-COO^-$ stretch, the $-NH_3^+$ deformational mode, and the C=C vibrations in AmB chromophores (Gagoś and Arczewska 2010). It is evident that the substantial increase in the intensity of this band is only observed at pH 7. This effect should be interpreted as aggregation via chromophores both in the horizontal and vertical orientation of AmB molecules. Interestingly, other spectroscopic techniques, for example resonance light scattering (RLS), also indicate this type of aggregation (Gagoś et al. 2008a; Gagoś et al. 2001). Similar results were obtained during compression of monolayers formed from AmB dissolved in mixtures of 2-propanol–water (4:6) at constant pH (Gagoś and Arczewska 2010; Gagoś et al. 2008a).

The bands centred in the range 1,300–1,200 cm^{-1} are associated with C–O stretch in the ester group and –OH bending in the carboxyl group. The broadening of this region seems to confirm association as a result of reorientation of AmB molecules on the surface, particularly at neutral pH. The band centred at 1,109 cm^{-1} is related to the rocking vibration of the $–NH_3^+$ group and is intense at low pH and high surface pressure (Fig. 3b). The appearance of this band is connected with the formation of hydrogen bonds between AmB molecules in aggregates. The band centred at 1,191 cm^{-1} (panel B, 20 mN/m) is typical of the vibrations of C–O. We were especially interested in the band at 1,010 cm^{-1}, because of its appearance both in the FTIR and Raman spectra of AmB and other polyenes (Bunow and Levin 1977; Colline et al. 1985; Espuelas et al. 1997; Gagoś and Arczewska 2010, 2011; Gagoś et al. 2011; Iqbal and Weidekamm 1979; Lewis et al. 1988; Ridente et al. 1995; Rimai et al. 1973; Schwartzman et al. 1978). The absorbance of this band (panels A, B) increases as pH is reduced; this is connected with changes in the distance between AmB chromophores which lead to association processes. This band is also assigned to the C–C vibrations of the C–C–H group coupled with the bending distortion of C=C–C in the chromophore of AmB (Bunow and Levin 1977; Colline et al. 1985; Mendelsohn and Van Holten 1979; Ridente et al. 1995; Rimai et al. 1973). The origin of this band is skeletal vibrations of C–C–H combined with changes in the chromophore chain (Gagoś and Arczewska 2011). The band centred at 1,070 cm^{-1} corresponds to the valence vibrations of the C–O bond in the alcohol fragment of the AmB molecule.

The decrease in absorbance with a maximum at approximately 3,150 cm^{-1} represents a complex superposition of valence of the N–H group and –OH stretching vibrations at high pH, suggesting this band is most probably associated with the amino group vibration. Horizontally oriented AmB molecules on the water surface (5 mN/m) could interact via –OH groups. At pH 7, strong, broad bands centred at ca 3,318 cm^{-1} (5 mN/m) and 3,376 cm^{-1} (20 mN/m) are assigned to valence vibrations of the –OH in hydrogen-bonded groups. The vibrations of the $–NH_3^+$ groups give rise to a characteristic band with a maximum at approximately 3,020 cm^{-1} (both panels). The band centred at 2,626 cm^{-1} (panel A, pH 11) is related to the asymmetrical and symmetrical vibrations of the $–NH_2$ group. This band decreases in intensity at low pH and at high surface pressure (panel B, 20 mN/m). This effect is probably related to changes in the orientation of the amino sugar group (mycosamine) (Gagoś and Arczewska 2010). It is known that a decrease in pH induces changes in electronic absorption spectra and aggregation of AmB (Gagoś et al. 2008a). At high surface pressure, the intensity of the band typical of dimers (3,376 cm^{-1}) formed via carboxyl groups is increased. Taking into account the steric properties of the AmB molecule, it is worth considering the H (*card pack*) types of dimers that are formed as a consequence of chromophore–chromophore interactions (Gagoś et al. 2001; Kasha 1963; Kasha et al. 1965).

It is known that AmB molecules form molecular aggregates at pH 7. Additionally, at high surface pressure, ca 20 mN/m, the vertically oriented molecules are able to form porous structures. At the same surface pressure but at higher pH (11), no changes in FTIR spectra characteristic of aggregation processes (despite the vertically oriented AmB) are observed, especially for the band centred at approximately 1,010 cm^{-1}. Interestingly, the weak absorption of valence vibration of hydrogen-bonded OH groups observed at pH 11 supports these results.

AmB interactions with DPPC lipid monolayers containing cholesterol and ergosterol

The ATR-FTIR spectroscopic studies of the molecular organization of AmB at different pH facilitated the analysis of the mechanisms of drug incorporation into the lipid monolayers containing sterols. As expected, only a small amount of AmB molecules should penetrate the subphase of the monolayer at relatively high starting surface pressure (22 mN/m). On the basis of these results, we can assume that, after the first injection of AmB into the subphase, the molecules are in the monomeric form (inset in Fig. 4) and are oriented horizontally to the surface. It has been suggested that both sterols—cholesterol and ergosterol—have a substantial effect on incorporation of AmB molecules (Gagoś et al. 2005). The significant increase in the surface pressure (ca 16 mN/m) after injection of AmB under the DPPC monolayer containing ergosterol (1:1) results in greater selectivity and much better incorporation of the antibiotic into the monolayer, compared with that containing cholesterol (Fig. 4). The AmB molecules interact with the polar heads of lipids and are localized in this part of the membrane. This kind of organization and high surface pressure in the monolayer (22 mN/m) can change the orientation of the antibiotic molecules from horizontal to vertical. Vertical orientation might lead to aggregation processes and the formation of AmB pores in the ergosterol-containing DPPC membrane (Gruszecki et al. 2002). The monolayers were deposited on to the surface of Ge plate by the Langmuir–Blodgett technique and monitored by means of ATR–FTIR spectroscopy. The purpose of this study was to analyse the interactions between AmB and the sterol-containing lipid membrane with cholesterol and ergosterol. Spectroscopic analysis of pure AmB has been reported elsewhere (Arczewska and Gagoś 2011; Espuelas et al. 1997; Schwartzman et al. 1978). Gagoś et al. (2005)

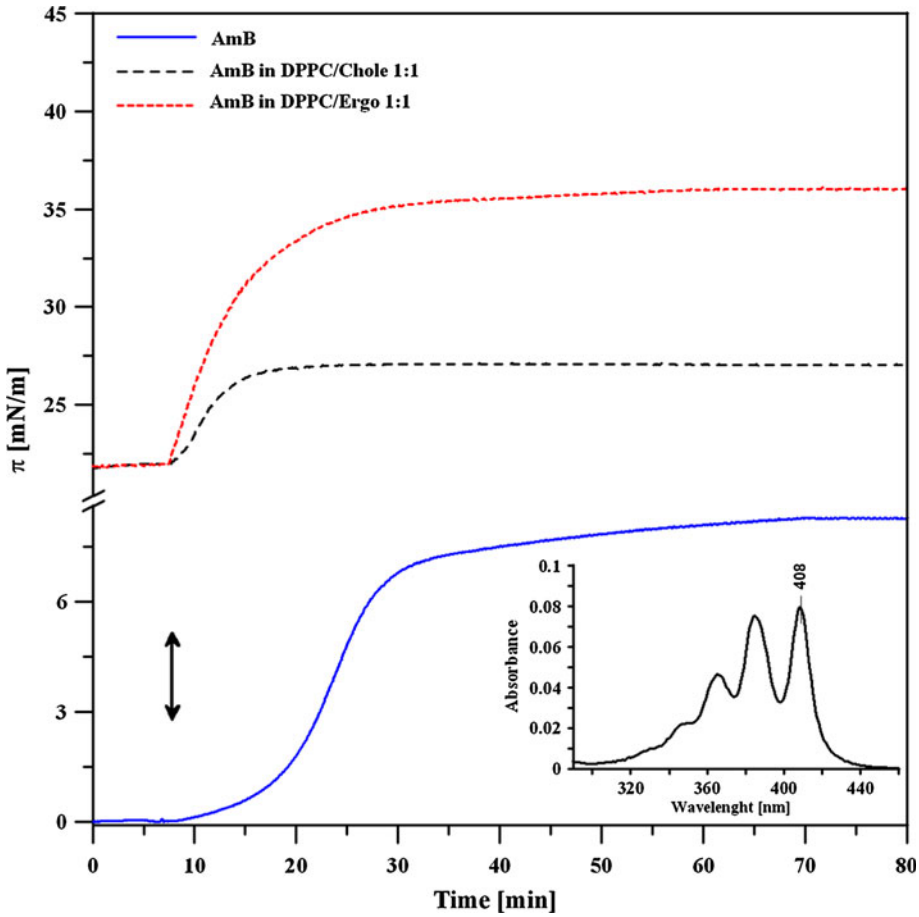

Fig. 4 Adsorption of AmB on the air–water subphase (*solid line*) and on the monomolecular layers formed by DPPC–cholesterol 1:1 (*dashed line*) and DPPC–ergosterol 1:1 (*dotted line*). Injection of AmB increased its concentration by 1 μM (see the *inset* of the electronic absorption spectrum of AmB in the monomeric form)

reported the effects of incorporation of AmB into lipid monolayers formed from DPPC and DPPC with cholesterol and ergosterol in 1:1 ratio. These findings were obtained under stabilized barrier conditions at 22 mN/m. To study the interactions between AmB and the sterol-containing lipid membrane, the monolayers in this work were deposited under the conditions of a totally packed system and at the maximum penetration surface pressure (ca 35 and 26 mN/m for lipid–ergosterol and lipid–cholesterol monolayers, respectively). The effects of injection of AmB solution into the subphase have been described in detail elsewhere (Gagoś et al. 2005). The final concentration of AmB was 1 μM.

The effect of sterols

The ATR–FTIR spectrum of AmB incorporated (under identical conditions and using the method discussed above) into DPPC monolayers containing cholesterol is shown in Fig. 5a. It is apparent the bands in the spectral region from 1,615 to 1,510 cm^{-1} assigned to the overlapping deformational vibrations of the $-NH_3^+$ group and the C=C bonds in the AmB chromophore are much less intense than for ergosterol. This is a consequence of previous considerations related to differences in the structures of the sterols. The more rigid molecule of ergosterol has a structure more complementary to that of AmB. The increase in intensity of this spectral region is because of the π–π^* electron interactions between the hydrophobic part of neighbouring AmB and ergosterol molecules (Baginski et al. 1994). Generally, it has been proved that the mixed lipid–cholesterol monolayers are characterized by significantly greater stability than the model lipid–ergosterol system (Dynarowicz-Latka et al. 2002). In this way, in FTIR spectra, different kinds of effects related to the mechanisms responsible for the molecular interactions between AmB molecules and sterol-rich lipid membranes might be observed.

The band with a maximum centred at 1,705 cm^{-1} (see the differential spectrum of AmB + DPPC + Chole in Fig. 6) is related to the stretching vibrations of –COOH in the hydrogen bonded (C=O···HO–) group whereas the band centred at approximately 1,641 cm^{-1} is assigned to the vibration of the $-COO^-$ (because the p*I* of AmB is approximately pH 6). The existence of these bands indicates their participation in the aggregation process. It is apparent the bands are shifted toward lower frequencies compared with those in the ergosterol-rich lipid membrane,

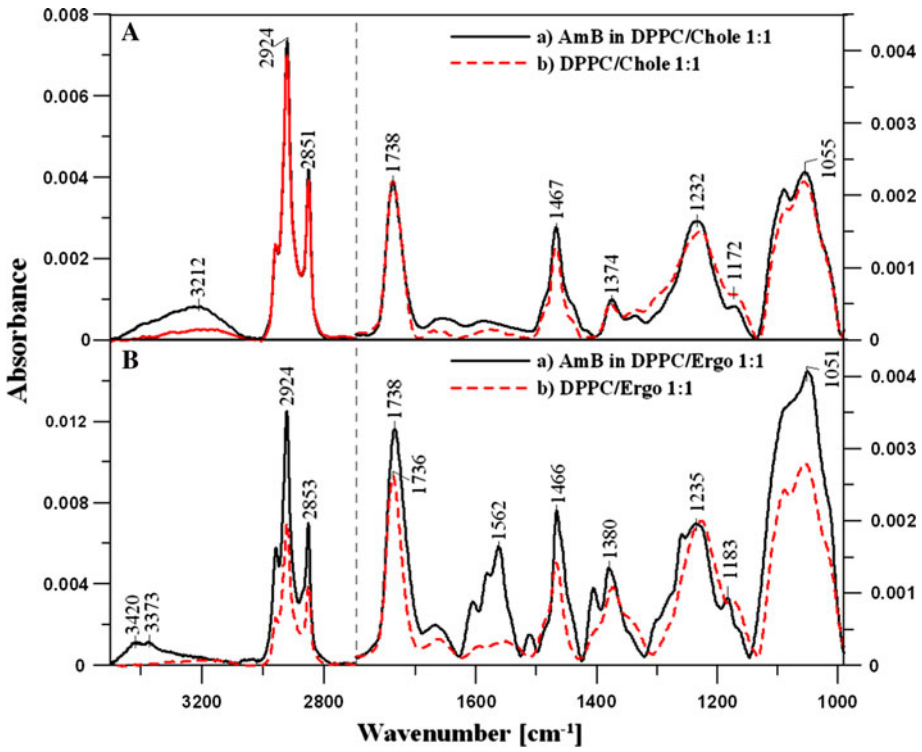

Fig. 5 ATR-FTIR absorption spectra of the monolayers formed by AmB with **a** DPPC–cholesterol (1:1) and **b** DPPC–ergosterol (1:1), and the spectrum of a pure lipid–sterol (1:1) monolayer (*dashed line*). Samples were deposited on the two sides of a Ge crystal plate at the maximum penetration surface pressure (ca 35 and 26 mN/m for lipid–ergosterol and lipid–cholesterol monolayers, respectively). Temperature, 24 °C

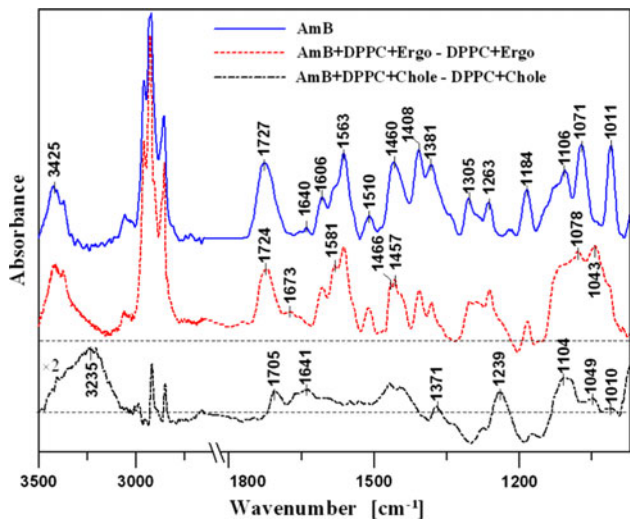

Fig. 6 The differential spectra obtained by subtraction of two-component monolayers composed of AmB and DPPC–sterol from pure DPPC–sterol samples (Fig. 5) in comparison with the infrared spectrum of pure AmB

which indicates a different kind of organization of AmB in these systems. The band with a maximum centred at 1,563 cm^{-1} (see the pure AmB and AmB + DPPC + Ergo spectra) results from the overlapping deformational vibrations of the $-NH_3^+$ group and weak stretching vibrations of the C=C bonds. This band is not observed for the cholesterol-containing DPPC because of the strong aggregation effect (Gruszecki et al. 2009). In the cholesterol-containing lipid membrane, hydrophobic interaction between AmB molecules is more likely than formation of lipid–sterol–AmB complexes. In agreement with the results published by Dynarowicz-Latka et al. (2002), lower AmB penetration into cholesterol-containing membranes compared with those composed of ergosterol can be explained by the greater stability of the DPPC–cholesterol complex. Analysis of values of the excess free energy of mixing for the cholesterol-rich lipid system revealed its packed structure, as a consequence of the existence of hydrogen bonds between the complex components (Dynarowicz-Latka et al. 2002).

In contrast, the process of incorporation of AmB into the ergosterol-containing lipid monolayer is known to be the most efficient (Baginski et al. 1989; Charbonneau et al. 2001; Dynarowicz-Latka et al. 2002; Gagoś et al. 2005). The FTIR differential spectrum presented in Fig. 6 illustrates the effect of the functional groups of AmB on the process of its incorporation into the ergosterol-rich lipid monolayers. Interestingly, the differential spectrum of ergosterol-containing lipid monolayer with incorporating AmB molecules is very similar to the FTIR spectrum of pure AmB. The strong intensity of the 1,563 cm^{-1} band indicates a larger number of molecules incorporated into the lipid membrane containing ergosterol. However, in the case of the carbonyl stretching band centred at 1,727 cm^{-1} (IR spectrum of pure AmB injected under the water surface; Figs. 4, 6), the presence of ergosterol in lipid monolayers causes a shift to lower frequencies of

approximately 3 cm^{-1}. On the other hand, the stretching vibrations of the C=O group are a superposition of component bands corresponding to *sn*–1 and *sn*–2 carbonyl groups in the lipid ester (Lewis et al. 1994a, b). Its shift suggests involvement of carbonyl groups in the process of interaction, especially via hydrogen bonding of the *sn*–2 carbonyl group with the AmB molecule (C=O···HO–). A more precise explanation may be based on the polarity effect, assuming that the *sn*–2 carbonyl group is closer to the PO_2^- group. Interaction of AmB molecules with the PO_2^- group was observed as spectral changes in the band centred at ca 1,260 cm^{-1}. It is suggested that the location of AmB molecules in the polar zone of the membrane also affects the *sn*–2 carbonyl group. The bands centred at 1,466 cm^{-1} and at 1,457 cm^{-1} (Fig. 6) are characteristic os scissoring deformation vibrations of the methylene group. The changes in the positions of these bands are indicative of the effect of AmB on the hydrophobic part of the membrane, for example by conformational change of lipid alkyl chains (*gauche–trans*) (Lewis et al. 1994a). A symmetrical deformation vibration of the methyl group (called "umbrella") is manifested in the spectrum as an absorption band near 1,380 cm^{-1}. The possibility of forming kink conformers (*gauche–trans–gauche*) is indicated by the appearance of a band centred at 1,371 cm^{-1}, especially for the cholesterol-containing membrane. In the cholesterol-containing lipid membrane (Fig. 6) there are two intense bands centred at 1,239 and 1,104 cm^{-1} characteristic of the PO_2^- group and the skeletal vibrations of C–O–P–O–C in DPPC. Additionally, the spectral features from the region between 2,800 and 3,000 cm^{-1} associated with the methylene symmetric and antisymmetric stretching modes are very strong in the presence of ergosterol in the lipid monolayer with AmB. As is apparent from Fig. 5b, the increased intensity of two bands at 2,853 and 2,924 cm^{-1} corresponding to symmetric and antisymmetric modes, respectively, are in agreement with the presence of disordered areas with a large number of gauche defects. The broad band in the region between 3,000 and 3,500 cm^{-1} is associated with the formation of hydrogen bonds between AmB and the sterol-containing lipid membrane. This effect is especially clear for the membrane containing cholesterol as a spectral red shift from 3,425 to 3,235 cm^{-1} and broadening of this band.

Conclusions

Changes in the ATR–FTIR absorption spectra in pH-dependent AmB monolayers prove involvement of carboxylate and ammonium groups in creation of associated forms of AmB. The net charge of AmB is of crucial importance in the changes in the limiting molecular area. In the basic subphase, the isotherms of AmB have a tendency to increase the expanded region and not to reach a real collapse, because of the high solubility of the molecules under these conditions. FTIR spectral changes induced by reorientation of the molecules are not as strong in the pH range 11–7. These findings indicate that the $–COO^-$ and $–NH_3^+$ groups are most important in the formation of associated structures. This might be crucial in understanding the interactions between AmB and sterol-rich systems at the molecular level, especially in the cholesterol-rich membrane. Comparison of the differential FTIR spectra of the monolayers reveals AmB is incorporated into ergosterol-rich membranes with greater selectivity. Our results confirm the existence of strong hydrophobic interactions between AmB and ergosterol-containing membranes compared with those composed of cholesterol. Lower penetration of AmB into cholesterol-containing membranes can be explained on the basis of the formation of stable lipid–sterol–AmB complexes.

Acknowledgments This research was financed by the Ministry of Education and Science of Poland from the budget funds for science in the years 2008–2011 within the research project N N401 015035.

References

Arczewska M, Gagoś M (2011) Molecular organization of antibiotic amphotericin B in dipalmitoylphosphatidylcholine monolayers induced by K(+) and Na(+) ions: the Langmuir technique study. Biochim Biophys Acta 1808:2706–2713

Baginski M, Borowski E (1997) Distribution of electrostatic potential around amphotericin B and its membrane targets. Theochem J Mol Struct 389:139–146

Baginski M, Tempczyk A, Borowski E (1989) Comparative conformational analysis of cholesterol and ergosterol by molecular mechanics. Eur Biophys J 17:159–166

Baginski M, Bruni P, Borowski E (1994) Comparative analysis of the distribution of the molecular electrostatic potential for cholesterol and ergosterol. Theochem J Mol Struct 311:285–296

Baran M, Mazerski J (2002) Molecular modelling of membrane sterols with the use of the GROMOS 96 force field. Chem Phys Lipids 120:21–31

Baran M, Borowski E, Mazerski J (2009) Molecular modeling of amphotericin B-ergosterol primary complex in water II. Biophys Chem 141:162–168

Barwicz J, Tancrede P (1997) The effect of aggregation state of amphotericin-B on its interactions with cholesterol- or ergosterol-containing phosphatidylcholine monolayers. Chem Phys Lipids 85:145–155

Bonilla-Marin M, Moreno-Bello M, Ortega-Blake I (1991) A microscopic electrostatic model for the amphotericin B channel. Biochim Biophys Acta 1061:65–77

Brajtburg J, Bolard J (1996) Carrier effects on biological activity of amphotericin B. Clin Microbiol Rev 9:512

Bunow MR, Levin IW (1977) Vibrational Raman spectra of lipid systems containing amphotericin B. Biochim Biophys Acta 464:202–216

Charbonneau C, Fournier I, Dufresne S, Barwicz J, Tancrede P (2001) The interactions of amphotericin B with various sterols in

relation to its possible use in anticancer therapy. Biophys Chem 91:125–133

Clejan S, Bittman R (1985) Rates of amphotericin B and filipin association with sterols. A study of changes in sterol structure and phospholipid composition of vesicles. J Biol Chem 260: 2884–2889

Colline A, Bolard J, Chinsky L, Fang JR, Rinehart KL Jr (1985) Raman spectra of nystatin. Influence of impurities. J Antibiot (Tokyo) 38:181–185

Cotero BV, Rebolledo-Antunez S, Ortega-Blake I (1998) On the role of sterol in the formation of the amphotericin B channel. Biochim Biophys Acta 1375:43–51

De Kruijff B, Gerritsen WJ, Oerlemans A, Demel RA, van Deenen LL (1974) Polyene antibiotic-sterol interactions in membranes of *Acholeplasma laidlawii* cells and lecithin liposomes. I. Specificity of the membrane permeability changes induced by the polyene antibiotics. Biochim Biophys Acta 339:30–43

Dynarowicz-Latka P, Seoane R, Minones J Jr, Velo M, Minones J (2002) Study of penetration of amphotericin B into cholesterol or ergosterol containing dipalmitoyl phosphatidylcholine Langmuir monolayers. Colloids Surf B 27:249–263

Espuelas MS, Legrand P, Irache JM, Gamazo C, Orecchioni AM, Devissaguet J-P, Ygartua P (1997) Poly(ε-caprolactone) nanospheres as an alternative way to reduce amphotericin B toxicity. Internat J Pharmaceut 158:19–27

Fournier I, Barwicz J, Tancrede P (1998) The structuring effects of amphotericin B on pure and ergosterol- or cholesterol-containing dipalmitoylphosphatidylcholine bilayers: a differential scanning calorimetry study. Biochim Biophys Acta 1373:76–86

Gagoś M, Arczewska M (2010) Spectroscopic studies of molecular organization of antibiotic amphotericin B in monolayers and dipalmitoylphosphatidylcholine lipid multibilayers. Biochim Biophys Acta 1798:2124–2130

Gagoś M, Arczewska M (2011) Influence of K+ and Na+ ions on the aggregation processes of antibiotic amphotericin B: electronic absorption and FTIR spectroscopic studies. J Phys Chem B 115:3185–3192

Gagoś M, Koper R, Gruszecki WI (2001) Spectrophotometric analysis of organisation of dipalmitoylphosphatidylcholine bilayers containing the polyene antibiotic amphotericin B. Biochim Biophys Acta 1511:90–98

Gagoś M, Gabrielska J, Dalla Serra M, Gruszecki WI (2005) Binding of antibiotic amphotericin B to lipid membranes: monomolecular layer technique and linear dichroism-FTIR studies. Mol Membr Biol 22:433–442

Gagoś M, Herec M, Arczewska M, Czernel G, Dalla Serra M, Gruszecki WI (2008) Anomalously high aggregation level of the polyene antibiotic amphotericin B in acidic medium: implications for the biological action. Biophys Chem 136:44–49

Gagoś M, Czernel G, Kaminski DM, Kostro K (2011) Spectroscopic studies of amphotericin B-Cu(2+) complexes. Biometals 24:915–922

Gold W, Stout HA, Pagano JF, Donovick R (1956) Amphotericins A and B, antifungal antibiotics produced by a Streptomycete. I. In vitro studies. Antibiot Ann 3:579–585

Gruszecki WI, Gagos M, Kernen P (2002) Polyene antibiotic amphotericin B in monomolecular layers: spectrophotometric and scanning force microscopic analysis. FEBS Lett 524:92–96

Gruszecki WI, Luchowski R, Gagoś M, Arczewska M, Sarkar P, Hereć M, Mysliwa-Kurdziel B, Strzalka K, Gryczynski I, Gryczynski Z (2009) Molecular organization of antifungal antibiotic amphotericin B in lipid monolayers studied by means of Fluorescence Lifetime Imaging Microscopy. Biophys Chem 143:95–101

Hamilton-Miller JM (1974) Fungal sterols and the mode of action of the polyene antibiotics. Adv Appl Microbiol 17:109–134

Hartsel SC, Hatch C, Ayenew W (1993) How does amphotericin B work?: studies on model membrane systems. J Liposome Res 3:377–408

Herve M, Debouzy JC, Borowski E, Cybulska B, Gary-Bobo CM (1989) The role of the carboxyl and amino groups of polyene macrolides in their interactions with sterols and their selective toxicity. A ^{31}P-NMR study. Biochim Biophys Acta 980:261–272

Iqbal Z, Weidekamm E (1979) Pre-resonance Raman spectra and conformations of nystatin in powder, solution and phospholipid-cholesterol multilayers. Biochim Biophys Acta 555:426–435

Kasha M (1963) Energy transfer mechanisms and the molecular exciton model for molecular aggregates. Radiat Res 20:55–71

Kasha M, Rawls HR, Ashraf El-Bayoumi M (1965) The exciton model in molecular spectroscopy. Pure Appl Chem 11:371–392

Lewis EN, Kalasinsky VF, Levin IW (1988) Quantitative determination of impurities in polyene antibiotics: Fourier transform Raman spectra of nystatin, amphotericin A, and amphotericin B. Anal Chem 60:2306–2309

Lewis RN, McElhaney RN, Monck MA, Cullis PR (1994a) Studies of highly asymmetric mixed-chain diacyl phosphatidylcholines that form mixed-interdigitated gel phases: Fourier transform infrared and 2H NMR spectroscopic studies of hydrocarbon chain conformation and orientational order in the liquid-crystalline state. Biophys J 67:197–207

Lewis RN, McElhaney RN, Pohle W, Mantsch HH (1994b) Components of the carbonyl stretching band in the infrared spectra of hydrated 1,2-diacylglycerolipid bilayers: a reevaluation. Biophys J 67:2367–2375

Mazerski J, Grzybowska J, Borowski E (1990) Influence of net charge on the aggregation and solubility behaviour of amphotericin B and its derivatives in aqueous media. Eur Biophys J 18:159–164

Mazerski J, Bolard J, Borowski E (1995) Effect of the modifications of ionizable groups of amphotericin B on its ability to form complexes with sterols in hydroalcoholic media. Biochim Biophys Acta 1236:170–176

Mendelsohn R, Van Holten RW (1979) Zeaxanthin ([3R,3′R]-beta, beta-carotene-3-3′diol) as a resonance Raman and visible absorption probe of membrane structure. Biophys J 27:221–235

Minones J Jr, Carrera C, Dynarowicz-Łątka P, Minones J, Conde O, Seoane R, Rodriguez Patino JM (2001) Orientational changes of amphotericin B in Langmuir monolayers observed by Brewster angle microscopy. Langmuir 17:1477–1482

Paquet MJ, Fournier I, Barwicz J, Tancrede P, Auger M (2002) The effects of amphotericin B on pure and ergosterol- or cholesterol-containing dipalmitoylphosphatidylcholine bilayers as viewed by 2H NMR. Chem Phys Lipids 119:1–11

Readio JD, Bittman R (1982) Equilibrium binding of amphotericin B and its methyl ester and borate complex to sterols. Biochim Biophys Acta 685:219–224

Rey-Gomez-Serranillos I, Dynarowicz-Łątka P, Minones J Jr, Seoane R (2001) Desorption of amphotericin B from mixed monolayers with cholesterol at the air/water interface. J Colloid Interface Sci 234:351–355

Ridente Y, Aubard J, Bolard J (1995) Surface-enhanced resonance Raman and circular dichroism spectra of amphotericin B and its methylester derivative in silver colloidal solutions. Biospectroscopy 2:1–8

Rimai L, Heyde ME, Gill D (1973) Vibrational spectra of some carotenoids and related linear polyenes. A Raman spectroscopic study. J Am Chem Soc 95:4493–4501

Saint-Pierre-Chazalet M, Thomas C, Dupeyarat M, Gary-Bobo CM (1988) Amphotericin B-sterol complex formation and competition with egg phosphatidylcholine: a monolayer study. Biochim Biophys Acta 944:477–486

Schwartzman G, Asher I, Folen V, Brannon W, Taylor J (1978) Ambiguities in IR and X-ray characterization of amphotericin B. J Pharm Sci 67:398–400

Seoane JR, Vila Romeu N, Miñones J, Conde O, Dynarowicz P, Casas M (1997) The behavior of amphotericin B monolayers at the air/water interface. Prog Colloid Polym Sci 105:173–179

Seoane JR, Minones J, Conde O, Casas M, Iribarnegaray E (1998) Molecular organisation of amphotericin B at the air-water interface in the presence of sterols: a monolayer study. Biochim Biophys Acta 1375:73–83

Sternal K, Czub J, Baginski M (2004) Molecular aspects of the interaction between amphotericin B and a phospholipid bilayer: molecular dynamics studies. J Mol Model (Online) 10:223–232

Sykora JC, Neely WC, Vodyanoy V (2004) Solvent effects on amphotericin B monolayers. J Colloid Interface Sci 269:499–502

Zotchev SB (2003) Polyene macrolide antibiotics and their applications in human therapy. Curr Med Chem 10:211–223